ELSEVIER

Journal of Molecular Catalysis A: Chemical 106 (1996) 93–102

JOURNAL OF MOLECULAR CATALYSIS A: CHEMICAL

Surface structures of supported tungsten oxide catalysts under dehydrated conditions

Du Soung Kim [1], Marlene Ostromecki, Israel E. Wachs *

Zettlemoyer Center for Surface Studies, Department of Chemical Engineering, Lehigh University, Bethlehem, PA 18015, USA

Received 28 February 1995; accepted 21 July 1995

Abstract

The molecular structures of the WO_3/support (Al_2O_3, TiO_2, Nb_2O_5, ZrO_2, SiO_2, and MgO) catalysts under in situ dehydrated conditions have been investigated by Raman spectroscopy. The series of catalysts was synthesized by the aqueous incipient wetness method. The WO_3/support catalysts, with the exception of the WO_3/SiO_2 and WO_3/MgO catalysts, possess a highly distorted, octahedrally coordinated surface tungsten oxide species with one short W=O bond (mono-oxo tungsten oxide species) at high surface coverages. The WO_3/SiO_2 catalysts exhibit strong Raman features of crystalline WO_3 particles due to the relative low density and reactivity of the surface hydroxyl groups. The WO_3/MgO catalysts possess non-stoichiometric compounds, $Mg_x(WO_4)_y$ and $Ca_x(WO_4)_y$, at low tungsten oxide contents and crystalline $MgWO_4$ and $CaWO_4$ at high tungsten oxide contents. This result is attributed to the high aqueous solubility of MgO as well as the CaO impurity and the strong acid–base interaction between WO_4^{2-} with $Mg(OH)_2$ and $Ca(OH)_2$. The current findings for supported tungsten oxide catalysts parallel the previous findings for supported molybdenum oxide catalysts and reflect the similar surface structural chemistry of these two oxides.

1. Introduction

Supported tungsten oxide catalysts are widely used for metathesis and isomerization of alkenes, dehydrogenation of alcohols, and hydrodesulfurization and hydrocracking of heavy fractions in the petroleum industry [1–7]. In addition, the WO_3 component is added to the V_2O_5/TiO_2 catalyst for the selectively catalytic reduction (SCR) of NO_x by NH_3 due to its high thermal stability and low SO_2 oxidation activity [8,9]. The industrial importance of supported tungsten oxide catalysts has resulted in a large number of studies concerning their surface properties [10–29] and catalysis [1–9].

The major structural information concerning the surface tungsten oxide species on oxide supports has been derived from Raman spectroscopy because of its ability to discriminate between different tungsten oxide species that may simultaneously be present in the catalysts. The majority of the previous Raman studies on supported tungsten oxide catalysts were performed under ambient conditions where moisture is present on the catalyst surface [9–19]. Relatively few Raman spectroscopic studies have been reported under in situ dehydrated

* Corresponding author.

[1] Present address: Research and Development Division, Daelim Engineering Co., Ltd. #17-5, Yoido-dong, Yongdungpo-ku, Seoul, 150-010, South Korea.

SSDI 1381-1169(95)00186-7

conditions, where the adsorbed moisture is removed from catalysts [27–31]. It is generally accepted that the terminal W=O bond of the surface tungsten oxide species shifts to the higher wavenumber region upon dehydration at elevated temperature. The assignment of the Raman band shift upon dehydration is still the subject of debates. Therefore, a systematic investigation is required to better understand the detailed surface structures of the tungsten oxide species on oxide supports.

Most of the previous in situ Raman spectroscopic studies have been devoted to examining the molecular structures of surface tungsten oxide supported on a few oxide supports (Al_2O_3 and TiO_2) and limited surface coverage. Therefore, this is the first systematic investigation of the molecular structures of surface tungsten oxide species on different oxide supports at different tungsten oxide contents under in situ dehydrated conditions. The present investigation focuses on the surface structure of the tungsten oxide species on the oxide supports Al_2O_3, TiO_2, Nb_2O_5, ZrO_2, SiO_2, and MgO. These oxide supports were chosen because of their widely varying surface characteristics and industrial applications.

2. Experimental

2.1. Catalyst preparation

A series of the supported tungsten oxide catalysts were prepared by incipient-wetness impregnation method with an aqueous solution of ammonium metatungstate ($(NH_4)_6H_2W_{12}O_{40}$). The support materials used in this investigation were Al_2O_3 (Harshaw, 180 $m^2\ g^{-1}$), TiO_2 (Degussa P-25 , anatase/rutile = 66/34, 55 $m^2\ g^{-1}$), ZrO_2 (Degussa, 39 $m^2\ g^{-1}$), and SiO_2 (Cab-O-Sil, 300 $m^2\ g^{-1}$). The Nb_2O_5 support (120 $m^2\ g^{-1}$) was prepared by the dehydration of hydrated niobium oxide [$Nb_2O_5 \cdot nH_2O$, Niobium Products Co.] in flowing O_2 at 393 K for 24 h. The MgO support (80 $m^2\ g^{-1}$) was prepared by the dehydration of magnesium hydroxide [$Mg(OH)_2$, Fluka Chemical Co.] in flowing O_2 at 973 K for 2 h. After impregnation, the wet samples were initially dried at room temperature for 16 h, further dried at 383 K for 16 h, and then calcined at 773 K for 16 h.

2.2. Raman spectroscopy

The Raman spectra of the supported tungsten oxide catalysts were obtained with an Ar^+ ion laser (Spectra Physics, Model 1877) delivering about 15–40 mW of incident radiation. The excitation line of the laser was 514.5 nm. The scattered radiation from the sample was directed into an optichannel multichannel analyzer with a photodiode array cooled thermoelectrically to 243 K (Princeton Applied Research, OMA III, Model 1463). The in situ Raman spectrometer was equipped with an in situ cell where the temperature and gaseous environment could be controlled. Prior to measurement, the catalysts were dehydrated at 773 K for 1 h in flowing O_2 and the in situ Raman spectra were collected at room temperature. Ultra-high purity, hydrocarbon free O_2 (Linde gas) was purged through the cell during the acquisition of the Raman spectra.

3. Results

3.1. WO_3/Al_2O_3 catalysts

The in situ Raman spectra of the WO_3/Al_2O_3 catalysts under dehydrated conditions are presented in Fig. 1. The 5% WO_3/Al_2O_3 catalyst possesses Raman bands at 1005, ~880, and ~300 cm^{-1} which are assigned to symmetric stretching mode of the terminal W=O, asymmetric mode of the W–O–W, and bending mode of the W=O bonds of the surface tungsten oxide species, respectively. The weak Raman bands at ~590 and ~215 cm^{-1}, which appear at coverages above 5%, are assigned to the symmetric and bending modes of the W–O–W bonds of the surface tungsten oxide species,

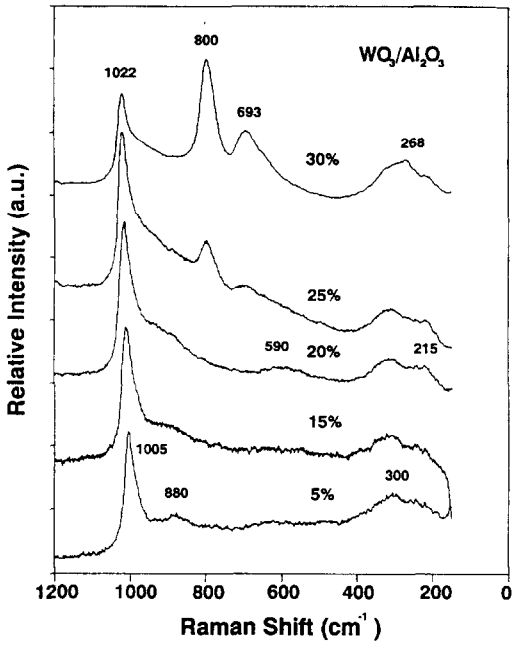

Fig. 1. The in situ Raman spectra of the WO_3/Al_2O_3 catalysts under dehydrated conditions.

respectively. The Raman band due to the terminal W=O bond of the surface tungsten oxide species shifts to the high wavenumber region, from 1005 to 1022 cm^{-1}, with increasing tungsten oxide content. The Raman bands at ~ 880, ~ 590, and ~ 215 cm^{-1} increase in intensity with increasing tungsten oxide content. The 25% WO_3/Al_2O_3 catalyst also exhibits very weak Raman bands at 800 and 693 cm^{-1} that are characteristic of microcrystalline WO_3 particles that did not completely disperse. The 30% WO_3/Al_2O_3 catalyst exhibits stronger Raman features due to crystalline WO_3 particles at 800, 693, and 268 cm^{-1} and reveals that monolayer coverage is exceeded. Monolayer coverage is approximated at 28% WO_3/Al_2O_3.

3.2. WO_3/TiO_2 catalysts

The in situ Raman spectra of the WO_3/TiO_2 catalysts under dehydrated conditions are shown in Fig. 2. The strong support Raman features due to the TiO_2 limits the collection of the data below 700 cm^{-1}. The weak Raman band at 799 cm^{-1} is due to the first overtone of the 395 cm^{-1} band of TiO_2 (anatase). The WO_3/TiO_2 catalysts exhibit a Raman band at 1010 cm^{-1} for the symmetric stretching mode of the terminal W=O bond of the surface tungsten oxide species independent of the tungsten oxide content. The 10% WO_3/TiO_2 catalyst exhibits strong Raman bands due to crystalline WO_3 at 800 cm^{-1} as well as the surface tungsten oxide species at 1010 cm^{-1}.

3.3. WO_3/Nb_2O_5 catalysts

The in situ Raman spectra of the WO_3/Nb_2O_5 catalysts under dehydrated conditions are shown in Fig. 3. Raman bands due to the Nb_2O_5 support have been subtracted from the spectra for the sake of clarity. The weak and broad Raman bands at ~ 1018 and ~ 956 cm^{-1} are characteristic of the surface tungsten oxide species. The intensity of the Raman band at ~ 956 cm^{-1} increases with increasing tungsten oxide coverage. For the 15% WO_3/Nb_2O_5 catalyst, the weak and sharp Raman band appearing at ~ 800 cm^{-1} is characteristic of crystalline WO_3 particles. This suggests that monolayer coverage of the surface tungsten oxide overlayer

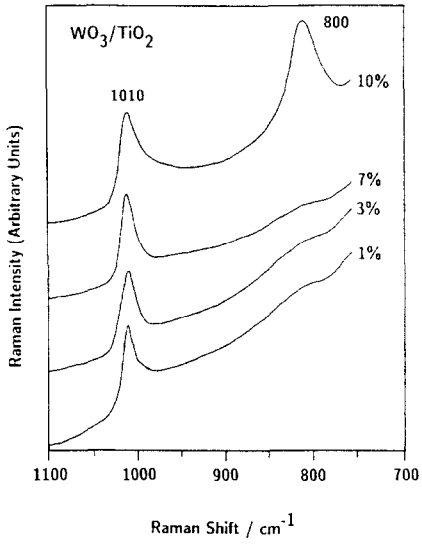

Fig. 2. The in situ Raman spectra of the WO_3/TiO_2 catalysts under dehydrated conditions.

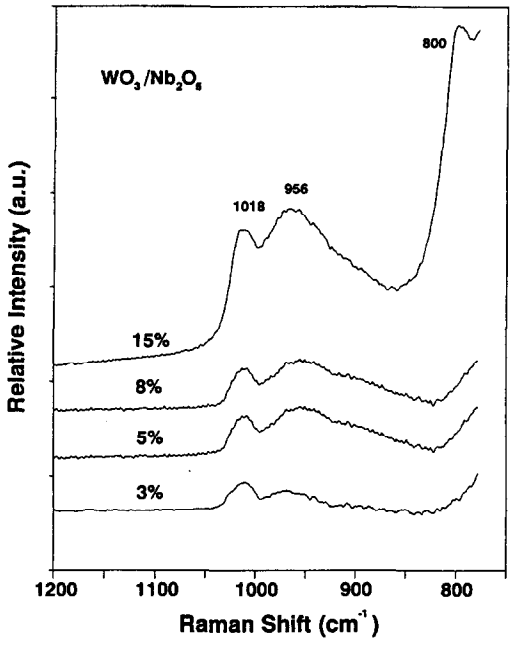

Fig. 3. The in situ Raman spectra of the WO_3/Nb_2O_5 catalysts under dehydrated conditions.

on Nb_2O_5 is achieved below 15% tungsten oxide coverage.

3.4. WO_3/ZrO_2 catalysts

The in situ Raman spectra of the WO_3/ZrO_2 catalysts under dehydrated conditions are shown in Fig. 4. The strong support Raman bands below 700 cm^{-1} interfere with the detection of diagnostic Raman bands for the other tungstate functionalities. The weak Raman band due to the ZrO_2 substrate is observed at 758–764 cm^{-1}. The 1% WO_3/ZrO_2 catalyst exhibits a Raman band at 1001 cm^{-1} for the symmetric stretching mode of the terminal W=O bond of the dehydrated surface tungsten oxide species. The 3% WO_3/ZrO_2 catalyst possesses Raman bands at 1009 and 804 cm^{-1} which are attributed to the symmetric stretch of the terminal W=O and asymmetric stretch of the W–O–W bonds, respectively. The symmetric stretching mode of the terminal W=O bond slightly shifts to lower wavenumbers 1004 cm^{-1}, while the asymmetric stretching mode of the W–O–W bond shifts to the higher wavenumber region ($\sim$ 875 cm^{-1}) and becomes broad with increasing the tungsten oxide content to 5%. Higher tungsten oxide loadings result in the formation of crystalline WO_3 particles which indicates that monolayer surface coverage has been exceeded.

3.5. WO_3/SiO_2 catalysts

The in situ Raman spectra of the WO_3/SiO_2 catalysts under dehydrated conditions are presented in Fig. 5. The 1% WO_3/SiO_2 catalyst exhibits Raman bands at $\sim$ 975, $\sim$ 800, $\sim$ 715, $\sim$ 600, $\sim$ 485, and $\sim$ 450 cm^{-1}. The Raman bands at $\sim$ 975, $\sim$ 800, $\sim$ 600, $\sim$ 485, and $\sim$ 450 cm^{-1} are characteristic of the SiO_2 support [32]. The Raman bands at $\sim$ 975 and $\sim$ 800 are also due to surface tungsten oxide species and crystalline WO_3, respectively, since the bands are sharper than those for only the SiO_2 support. The Raman band at $\sim$ 975 cm^{-1} is assigned to the symmetric stretching mode of the terminal W=O bond of the surface tungsten

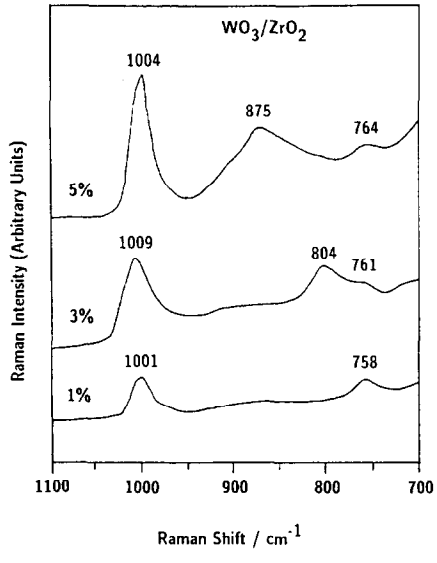

Fig. 4. The in situ Raman spectra of the WO_3/ZrO_2 catalysts under dehydrated conditions.

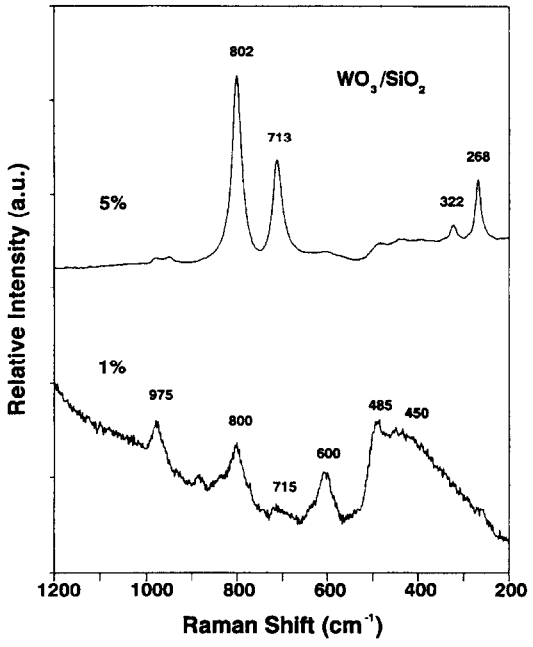

Fig. 5. The in situ Raman spectrum of the WO_3/SiO_2 catalysts under dehydrated conditions.

oxide species. The Raman bands at 800 and 715 cm^{-1} are due to crystalline WO_3 particles. The intensity of the bands due to the SiO_2 support decrease with increasing tungsten oxide content because of the stronger signals from the tungsten oxide component. The 5% WO_3/SiO_2 catalyst exhibits Raman bands at 802, 713, 322, and 268 cm^{-1} which are due to crystalline WO_3 particles.

3.6. WO_3/MgO catalysts

The in situ Raman spectra of the WO_3/MgO catalysts under dehydrated conditions are shown in Fig. 6. The 1% WO_3/MgO catalyst exhibits a strong Raman band at 895 cm^{-1} and weak Raman bands at ~ 1090, ~ 817, ~ 390, ~ 330, and ~ 275 cm^{-1}. The weak Raman bands at ~ 1090 and ~ 275 cm^{-1} are characteristic of a crystalline $CaCO_3$ impurity present in the MgO support [33]. The Raman bands at 895, ~ 817, ~ 390, and ~ 330 cm^{-1} are assigned to non-stoichiometric compounds of $Mg_x(WO_4)_y$ and $Ca_x(WO_4)_y$. Catalysts above 3% show Raman bands at ~ 915, ~ 330 and ~ 217 cm^{-1}, which are assigned to crystalline $CaWO_4$ [23,34,35]. The Raman band at ~ 915 cm^{-1} for the WO_3/MgO catalysts above 5% is also characteristic of crystalline $MgWO_4$ [23] because the additional Raman band at ~ 800 cm^{-1} due to crystalline $MgWO_4$ is present [23]. Crystalline $CaWO_4$ has strong Raman bands at 911 and 338 cm^{-1} and weak Raman bands at 834, 798, 400, 211, and 118 cm^{-1}. Crystalline $MgWO_4$ exhibits strong Raman bands at 911 and 800 cm^{-1} and weak Raman bands at 705, 545, 414, 345, and 271 cm^{-1}. The Raman bands due to the crystalline $CaWO_4$ and $MgWO_4$ increase at the expense of the bands at 1090, ~ 895, ~ 817, and ~ 275 cm^{-1} as the tungsten oxide content increases. The Raman band observed at ~ 968 cm^{-1} for the 5–12% WO_3/MgO catalysts is tentatively assigned to a mildly distorted terminal W=O bond of the surface tungsten oxide species.

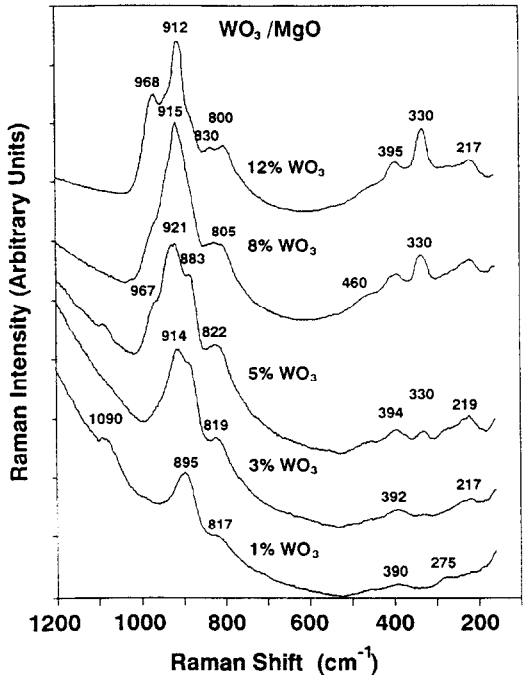

Fig. 6. The in situ Raman spectra of the WO_3/MgO catalysts under dehydrated conditions.

4. Discussion

Many previous studies have proposed that two-dimensional transition metal oxide overlayers are formed when one metal oxide component (i.e., V_2O_5, MoO_3, CrO_3, WO_3, Re_2O_7, Nb_2O_5, etc.) is deposited on a second metal oxide substrate (i.e., Al_2O_3, TiO_2, ZrO_2, SiO_2, etc.) [27,29–31,36,37]. However, it was generally accepted that the structures of the surface metal oxide species on oxide supports are not influenced by presence or absence of moisture [27,29–31]. However, recent characterization studies have demonstrated that quite different metal oxide species are formed on oxide supports upon dehydration by performing in situ nuclear magnetic resonance (NMR) [38,39], EXAFS/XANES [40], and Raman spectroscopic studies [28,40–43]. It was concluded from these investigations that under ambient conditions hydrated surface metal oxide species are present on the oxide support surface and are essentially in a solvated state. Consequently, the surface structures of the metal oxide species under ambient conditions are strongly dependent on the net surface pH at PZC (point of zero charge) [44,45]. Upon dehydration at elevated temperature, the hydrated surface metal oxide species are unstable and decompose to form dehydrated surface metal oxide species [28,40–43,46] by direct interaction with the surface OH groups of support (formation of Metal–O–Support bonds) [46]. Kim et al. have shown that for the MoO_3/TiO_2 [47] and CrO_3/SiO_2 [48] catalysts the dehydrated metal oxide species are formed upon dehydration above 573 K by combined Raman spectroscopic and thermal gravimetric studies. The above results suggest that the structural information of metal oxide species should be obtained under dehydrated conditions in order to investigate the relation between the surface structure–reactivity of supported metal oxide catalysts.

The present in situ Raman spectroscopy studies revealed that the WO_3/support (Al_2O_3, TiO_2, Nb_2O_5, and ZrO_2) catalysts possess a major Raman band at $\sim 1000–1020\ cm^{-1}$ due to the terminal W=O bond of the dehydrated tungsten oxide species. In addition, previous IR studies showed that the WO_3/Al_2O_3 and WO_3/TiO_2 catalysts exhibit an IR band due to the terminal W=O bond of the dehydrated surface tungsten oxide species at 1010–1022 [28,29,49] and 1015 cm^{-1} [49], respectively. The Raman and IR bands due to the terminal W=O bond, at corresponding tungsten oxide content, are observed at similar frequencies. The correspondence of the terminal W=O frequency in the Raman and IR spectra suggests that mono-oxo tungsten oxide species are present on the oxide support. If a di-oxo (O=W=O) tungsten oxide species were present, it should give rise to two Raman and IR bands due to the symmetric and asymmetric stretching modes of the O=W=O bond with different relative intensities and wavenumbers (30–50 cm^{-1} difference) [49–51]. Moreover, Horsley et al. [15] found with in situ XANES that the surface tungsten oxide species in WO_3/Al_2O_3 catalysts, calcined at 773 K, is predominantly present as a highly distorted, octahedrally coordinated tungsten oxide species at high tungsten oxide coverages and a distorted tetrahedral species at tungsten oxide coverages below 1/3 monolayer. Hilbrig et al. [52] found with in situ XANES that the surface tungsten oxide species of WO_3/TiO_2 catalysts, calcined at 673 K, is present as a distorted, pentahedral coordinated tungsten oxide species at high tungsten oxide coverages and a distorted tetrahedral species at tungsten oxide coverages below 1/3 monolayer. Hilbrig et al. [52] also predicted the same situation for tungsten oxide on Al_2O_3. These in situ XANES and Raman results suggest that the structure of the surface tungsten oxide species on Al_2O_3 and TiO_2 as well as Nb_2O_5 and ZrO_2 are a function of surface tungsten oxide coverage.

In addition to the major Raman band at $\sim 1000–1020\ cm^{-1}$, the tungsten oxide supported Nb_2O_5, ZrO_2, Al_2O_3, and TiO_2 catalysts also exhibit a weaker Raman band at $\sim 800–960$

cm^{-1}. This band increases in intensity with increasing tungsten oxide coverage in the order $Nb_2O_5 > ZrO_2 > Al_2O_3 > TiO_2$ which indicates the presence of a second tungsten oxide species. The Raman band at ~800–960 cm^{-1} is assigned to the asymmetric mode of a W–O–W linkage, suggesting the second tungsten oxide species consists of a surface polytungsten oxide species on the oxide support [28]. The Raman band at ~956 cm^{-1} of the WO_3/Nb_2O_5 catalysts is more intense than the Raman band at ~1018 cm^{-1} for tungsten oxide coverages above 3%. The Raman band at 804 cm^{-1} for the 3% WO_3/ZrO_2 catalyst becomes broadened and shifts to the higher wavenumber (875 cm^{-1}) region when the tungsten oxide coverage increases to 5%. For tungsten oxide contents above 5% WO_3/Al_2O_3, additional weak Raman bands are present at ~590 and 215 cm^{-1}. These bands increase as the band at ~880 cm^{-1} increases with tungsten oxide coverage and are assigned to the symmetric and bending modes of the W–O–W linkage, respectively. The WO_3/TiO_2 catalysts exhibit a very weak Raman band at ~880 cm^{-1} which suggests the surface tungsten oxide species is present as a less polymerized surface tungsten oxide species.

Silica supported metal oxides (MoO_3, V_2O_5, CrO_3, and WO_3) generally possess very poorly dispersed metal oxide phases that are present as corresponding crystalline metal oxide particles when prepared by impregnation or the incipient wetness method [42,43,48,53,54]. Recently, Ekerdt et al. [46,53] demonstrated that the preparation method and precursor are important parameters that control the dispersion of surface molybdenum and tungsten oxide species on SiO_2. They have successfully prepared highly dispersed MoO_3/SiO_2 and WO_3/SiO_2 catalysts up to 7.8 [46] and 9.6 wt% [55], respectively, without formation of crystalline MoO_3 and WO_3 by using a non-aqueous preparation method involving organometallic precursors. They [55] also reported that the surface tungsten oxide species on silica possesses an isolated, octahedrally coordinated tungsten oxide structure with one short W=O bond (ν_s(W=O): 982–984 cm^{-1}) regardless of the tungsten oxide content. The current studies confirm that aqueous preparation of WO_3/SiO_2 catalysts with ammonium metatungstate favors the formation of crystalline WO_3 particles. The 1% WO_3/SiO_2 catalysts contains both surface tungsten oxide species, Raman band at ~975 cm^{-1}, and crystalline WO_3 particles, Raman bands at ~800 and ~715 cm^{-1}. The 5% WO_3/SiO_2 catalyst is dominated by the strong Raman signals of the crystalline WO_3 particles and the surface tungsten oxide species are not detectable. Thus, the preparation method is responsible for controlling the dispersion of metal oxides on SiO_2.

The WO_3/MgO catalysts showed very different Raman features compared to the other supported tungsten oxide catalysts. The absence of the 980–1020 cm^{-1} Raman band due to the symmetric stretching mode of the terminal W=O bond for the dehydrated surface tungsten oxide species indicates that different tungsten oxide species are present on the MgO support. The Raman band at 968 cm^{-1} for the 5–12% WO_3/MgO catalysts is due to a mildly distorted W=O bond of the dehydrated surface tungsten oxide species since this band shifts upon hydration. Wang [29] and Kim et al. [42,55] have demonstrated that MgO and the CaO impurity are readily soluble in water and easily make a compound with MoO_4^{2-} (aq), CrO_4^{2-} (aq), ReO_4^- (aq), WO_4^{2-} (aq), and VO_4^{3-} (aq) during aqueous preparations. The formation of such compounds is strongly dependent on the pH of the impregnating solution, calcination temperature and time [42,55]. The Raman band positions for 1% WO_3/MgO catalyst does not correspond with the Raman bands of crystalline $CaWO_4$ and $MgWO_4$. The different Raman features for the 1% WO_3/MgO catalysts are attributed to the formation of a solid solution of tungsten oxide with the MgO support due to the strong acid–base interaction of WO_4^{2-} (aq) with MgO as well as nonstoichiometric compounds such as $Mg_x(WO_4)_y$. At high tungsten oxide

contents, both $CaWO_4$ and $MgWO_4$ compounds are present. A similar trend is observed for the magnesia supported V_2O_5, MoO_3, Re_2O_7, and CrO_3 catalysts [55,56].

Supported tungsten oxide and molybdenum oxide catalysts behave similarly on the oxide supports Al_2O_3, TiO_2, Nb_2O_5, ZrO_2, SiO_2, and MgO. The structures of the dehydrated surface tungsten and molybdenum oxide species on the oxide supports are both dependent on tungsten and molybdenum oxide [56–58] coverage, respectively. At low surface tungsten and molybdenum oxide coverages, a highly distorted, tetrahedral and isolated structure is dominant on the oxide supports Al_2O_3, TiO_2, Nb_2O_5, and ZrO_2. As the tungsten and molybdenum oxide contents approach monolayer coverage, polytungsten and polymolybdenum oxide species also appear on the supports with a highly distorted, octahedral mono-oxo structure. Both isolated surface tungsten and molybdenum oxide species and crystallites are present on SiO_2, and their relative populations depend on the specific preparation method. Magnesium oxide supported tungsten and molybdenum oxide catalysts possess both surface oxide species and compound with MgO and the CaO impurity. The analogous behavior of the supported tungsten oxide and molybdenum oxide catalysts reflects the similar solid state chemistry of the two oxides [57]. Also, the monolayer densities of the supported tungsten and molybdenum oxide catalysts [57] are very similar as shown in Tables 1 and 2, respectively. Since tungsten and molybdenum oxide supported MgO and SiO_2 catalysts form compounds and crystals at monolayer coverage, respectively, their monolayer densities are not listed in Tables 1 and 2.

Table 1
The surface density of supported WO_3 catalysts at monolayer coverage

Support	Surface area (m^2/g)	Monolayer loading (wt% WO_3)	Surface density (W/nm^2)
Al_2O_3	180	~ 28	4.0
TiO_2	55	~ 9	4.2
ZrO_2	39	~ 6	4.0
Nb_2O_5	120	~ 14	3.0

Table 2
The surface density of supported MoO_3 catalysts at monolayer coverage

Support	Surface area (m^2/g)	Monolayer loading (wt% MoO_3)	Surface density (Mo/nm^2)
Al_2O_3	180	~ 20	4.6
TiO_2	55	~ 6	4.6
ZrO_2	39	~ 4	4.3
Nb_2O_5	55	~ 6	4.6

5. Conclusion

A series of supported tungsten oxide catalysts on different oxide supports (Al_2O_3, TiO_2, Nb_2O_5, ZrO_2, SiO_2, and MgO) was structurally characterized by in situ Raman spectroscopy. The surface tungsten oxide species on Al_2O_3, TiO_2, Nb_2O_5, and ZrO_2 possess a highly distorted, octahedrally coordinated surface tungsten oxide structure with one short W=O bond (mono-oxo species) at high surface coverages. The extent of the polymerization of the surface tungsten oxide species is strongly dependent on the tungsten oxide coverage and the specific oxide support. At low surface coverages, an isolated, tetrahedral, coordinated surface tungsten oxide species appears to predominate. The WO_3/SiO_2 catalyst contains crystalline WO_3 because of the lower density and reactivity of the silica surface OH groups during the aqueous preparation method. The WO_3/MgO catalysts possess $MgWO_4$ and $CaWO_4$ compounds due to the high solubility of MgO and impurity CaO in aqueous solutions and the strong acid–base interaction between tungsten oxide and MgO/CaO. The presence of some surface tungsten oxide species on MgO was also detected. The current findings for supported tungsten oxide catalysts essentially follow the behavior previously found for the corresponding supported molybdenum oxide catalysts.

Acknowledgements

The financial support of Department of Energy, Basic Energy Sciences (program #DEFG02-93ER14350) is gratefully acknowledged.

References

[1] M. Ai, J. Catal., 49 (1977) 305.
[2] T. Yamaguchi, Y. Tanaka and K. Tanabe, J. Catal., 65 (1980) 442.
[3] A.J. Moffat, A. Clark and M.M. Johnson, J. Catal., 22 (1971) 379.
[4] W. Grunert, R. Feldhaus, K. Anders, E.S. Shpiro and K.M. Minachev, J. Catal., 120 (1989) 444.
[5] D.C. Grenobole and W. Weissman, US Pat. No. 4 233 (1980) 179.
[6] E. Ogata, Y. Kamiya and N. Ohta, J. Catal., 29 (1973) 296.
[7] H. Hattori, N. Asada and K. Tanabe, Bull Chem. Soc. Jpn., 51 (1978) 1704.
[8] M. Imanari, Y. Watanabe, S. Matsuda and F. Nakajima, in T. Seiyama and K. Tanabe (Eds.), Proceedings, 7th International Congress on Catalysis, Tokyo, 1980 p. 604. Kodansa/Elsevier, Tokyo/Amsterdam, 1981.
[9] S. Morikawa, K. Takahashi, J. Mogi and S. Kurita, Bull. Chem. Soc. Jpn., 55 (1982) 2254.
[10] J. Bernholc, J.A. Horsley, L.L. Murrell, L.G. Sherman and S. Soled, J. Phys. Chem., 91 (1987) 1526.
[11] A.J. van Roosmalen, D. Koster and J.C. Mol, J. Phys. Chem., 84 (1980) 3075.
[12] W. Grunert, E.S. Shpiro, R. Feldhaus, K. Anders, G.V. Antoshin and K.M. Minachev, J. Catal., 107 (1987) 522.
[13] I.E. Wachs, C.C. Chersich and J.H. Hardenbergh, Appl. Catal., 13 (1985) 335.
[14] F. Hilbrig, H.E. Gobel, H. Knozinger, H. Schmelz and B. Lengeler, J. Phys. Chem., 95 (1991) 6973.
[15] J.A. Horsley, I.E. Wachs, J.M. Brown, G.H. Via and F.D. Hardcastle, J. Phys. Chem., 91 (1987) 4014.
[16] J.C. Carver, I.E. Wachs and L.L. Murrell, J. Catal., 100 (1986) 500.
[17] S.S. Chan, I.E. Wachs, L.L. Murrell and N.C. Dispenziere, Jr., J. Catal., 92 (1985) 1.
[18] S.S. Chan, I.E. Wachs and L.L. Murrell, J. Catal., 90 (1984) 150.
[19] S. Soled, L.L. Murrell, I.E. Wachs, G.B. Mcvichel, S.S. Chan, N.C. Dispenziere and R.T.K. Baker, in R.K. Grasselli and J.F. Brazdil (Eds.), Solid State Chemistry in Catalysis, ACS Symposium Series 279, American Chemical Society, Washington, D.C., 1985, p. 165.
[20] S.S. Chan, I.E. Wachs, L.L. Murrell and N.C. Dispenziere, in S. Kaliaguine and A. Mahay (Eds.), Catalysis on the Energy Scene, Elsevier Science Publishers B.V., Amsterdam, 1984, p. 259.
[21] I.E. Wachs, F.D. Hardcastle and S.S. Chan, Spectroscopy, 1 (1986) 30.
[22] R. Thomas, F.P.J.M. Kerkhof, J.A. Moulijn, J. Madema and V.H.J. de Beer, J. Catal., 61 (1980) 559.
[23] R. Thomas, M.C. Mittelmeijer-Hazeleger, F.P.J.M. Kerkhof, J.A. Moulijn, J. Medema and V.H.J. de Beer, in H.F. Barry and P.C.H. Mitchell (Eds.), Proceedings, Climax Third International Conference on the Chemistry and Uses of Molybdenum, Climax Molybdenum Co., Ann Arbor, MI, 1979, p. 85.
[24] P. Tittarelli, A. Iannibello and P.L. Villa, J. Solid State Chem., 37 (1981) 95.
[25] R. Thomas, J.A. Moulijn and F.P.J.M. Kerkhof, Recl. Trav. Chem. Pays-Bas, 96 (1977) M134.
[26] G.C. Bond, J.P. Flamerz and L. van Wijk, Catal. Today, 1 (1987) 229.
[27] S.S. Chan, I.E. Wachs, L.L. Murrell, L. Wang and W.K. Hall, J. Phys. Chem., 88 (1984) 5831.
[28] (a) M.A. Vuurman, PhD Thesis, University of Amsterdam, 1992; (b) M.A. Vuurman and I.E. Wachs, J. Phys. Chem., 96 (1992) 5008; (c) M.A. Vuurman, I.E. Wachs and A.M. Hirt, J. Phys. Chem., 95 (1991) 9928.
[29] L. Wang, PhD Thesis, The University of Wisonsin, Milwaukee, WI, 1982.
[30] J.M. Stencel, L.E. Makovsky, J.R. Diehl and T.A. Sarkus, J. Raman Spectrosc., 25 (1984) 282.
[31] E. Payen, S. Kasztelan, J. Grimblot and J.P. Bonnell, J. Raman Spectrosc., 17 (1986) 233; J. Mol. Struct., 143 (1986) 259.
[32] D.R. Tallant, B.C. Bunker, C.J. Brinker and C.A. Balfe, Mater. Res. Symp. Proc., 73 (1986) 261.
[33] J.M. Jehng and I.E. Wachs, J. Phys. Chem., 95 (1991) 7373.
[34] (a) R.K. Khanna, W.S. Brower, B.R. Guscott and E.R. Lippincott, Journal of Research of the National Bureau of Standard-A. Physics and Chemistry, 72A (1968) 81; (b) R.K. Khanna and E.R. Lippincott, Spectrochim. Acta, 24A (1968) 905.
[35] S.P.S. Porto and J.F. Scott, Phys. Rev. 157 (1967) 716.
[36] L. Dixit, D.L. Gerrard and H. Bowley, Appl. Spectrosc. Rev., 22 (1986) 189.
[37] J.R. Bartlett and R.P. Coonet, in R.J.H. Clark and R.E., Hester (Eds.), Spectroscopy of Inorganic-Based Materials, Wiley, New York, 1987, p. 187.
[38] (a) H. Ekerdt and I.E. Wachs, J. Phys. Chem., 93 (1989) 6796; (b) H. Ekerdt, G. Deo, I.E. Wachs and A.M. Hirt, Colloids Surf., 45 (1990) 347.
[39] N. Das, H. Ekerdt, H. Hu, I.E. Wachs, J.F. Walzer and F.J. Feher, J. Phys. Chem., 97 (1993) 8240.
[40] M. de Boer, A.J. van Dillen, D.C. Koningsberger, J.W. Gues, M.A. Vuurman and I.E. Wachs, Catal. Lett., 11 (1991) 227.
[41] T. Machej, J. Haber, A.M. Turek and I.E. Wachs, Appl. Catal., 70 (1990) 115.
[42] (a) D.S. Kim, K. Segawa, T. Soeya and I.E. Wachs, J. Catal., 136 (1992) 539; (b) D.S. Kim and I.E. Wachs, J. Catal., 141 (1993) 419; (c) D.S. Kim and I.E. Wachs, J. Catal., 146 (1994) 268.
[43] G. Deo, PhD Thesis, Lehigh University, Bethlehem, PA, 1993.
[44] G. Deo and I.E. Wachs, J. Phys. Chem., 95 (1991) 5889.

[45] S.D. Kohler, J.G. Ekerdt, D.S. Kim and I.E. Wachs, Catal. Lett., 16 (1992) 231.
[46] R.D. Roark, S.D. Kohler, J.G. Ekerdt, D.S. Kim and I.E. Wachs, Catal. Lett., 16 (1992) 77.
[47] D.S. Kim and I.E. Wachs, to be submitted to Journal of Molecular Catalysis.
[48] D.S. Kim, J.M. Tatibouet and I.E. Wachs, J. Catal., 136 (1992) 209.
[49] G. Ramis, G. Busca, C. Christiani, L. Lietti, P. Forzatti and F. Bregani, Langmuir, 8 (1992) 1744.
[50] B. Soptrajanov, A. Nikolovskii and I. Petrov, Spetrochim. Acta A, 24 (1968) 1617.
[51] W. Levason, R. Narayanaswami, J.S. Ogden, A.J. Rest and J.W. Turff, J. Chem. Soc., Dalton Trans., 2009 (1982).
[52] F. Hilbrig, H.E. Gobel, H. Knozinger, H. Schmelz and B. Lengeler, J. Phys. Chem., 95 (1991) 6974.
[53] R. Thomas, M.C. Mittelmeijer-Hazeleger, F.P.D.J. Kerkhof, J.A. Moulijn, J. Medema and V.H.J. de Beer, in H.F. Barry and P.C.H. Mitchell (Eds.), Proceedings, 3rd Internatonal Climax Conference on the Chemistry and Usage of Molybdenum, Ann Arbor, MI, 1979, p. 85.
[54] C.C. Williams, J.G. Ekerdt, J.M. Jehng, F.D. Hardcastle, A.M. Turek and I.E. Wachs, J. Phys. Chem., 95 (1991) 8781.
[55] D.S. Kim and I.E. Wachs, unpublished results.
[56] S.R. Bare, S. Chang and M.A. Leugers, J. Phys. Chem., 96 (1992) 10358.
[57] H.H. Hu, PhD Thesis, Lehigh University, Bethlehem, PA, 1994.
[58] D.S. Kim, I.E. Wachs and K. Segawa, J. Catal., 146 (1994) 268.